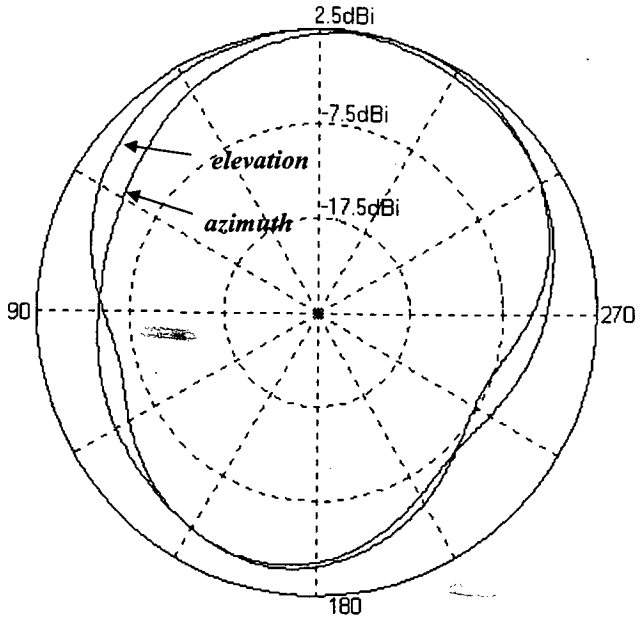

Figure 5 Measured radiation patterns for the phone in free space for two planes. The back of the phone is pointing towards 0° and the bottom of the phone towards 90° (the elevation cut and azimuth plane are shown by solid and dashed lines, respectively)

As stated previously, a lot of potential integrations are possible because the resonant frequency no longer depends on the shape or the material. In Table 1 we have a set of outer dimensions that have been used in other phone-integration cases, showing sets of dimensions that can fit more or less most of the applications.

CONCLUSION

We have proposed and demonstrated a compact antenna structure at GPS frequencies, which provides high isolation and efficiency suitable for mobile devices. The high isolation enables multiple configurations based on the same structure and makes integration more efficient. The antenna also presents extremely high out-of-band rejection.

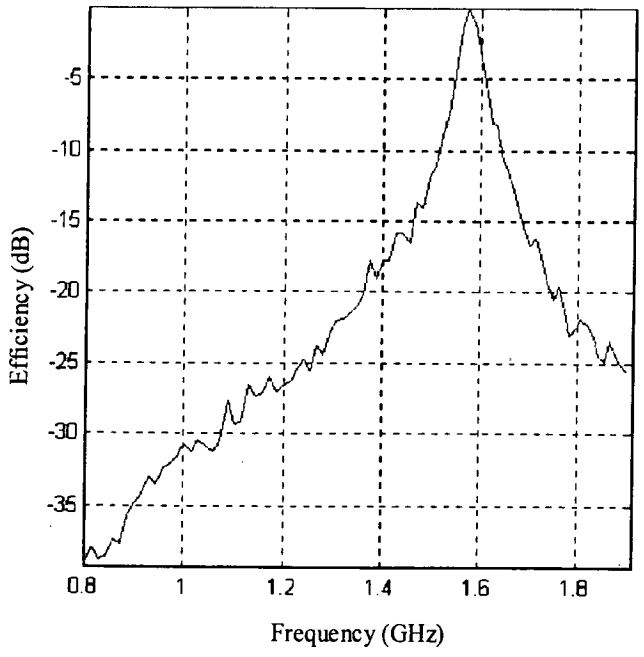

Figure 6 Normalized antenna efficiency (total power radiated) as a function of frequency over a broad band: 800 MHz to 1900 GHz

TABLE 1 Different Dimension Combinations Used to Obtain GPS Antennas

	Length (mm)	Width (mm)	Height (mm)
Antenna 1	25	12	2.5
Antenna 2	12	10	5.5
Antenna 3*	20	8	2.5
Antenna 4*	25	4	5

* Antennas 3 and 4 are on 3-mm legs in order to bridge components.

REFERENCES

1. W.L. Stutzman and G.A. Thiele, Antenna theory and design, 2nd ed., Wiley, New York, 1981.
2. C.R. Rowell and R.D. Murch, A Compact PIFA suitable for dual-frequency 900/1800-MHz operation, IEEE Trans Antennas Propagat 46 (1998), 596–598.

A K-BAND SUSPENDED MICROSTRIPLINE-FED LINEAR TAPERED SLOT ANTENNA AND ITS E-PLANE ARRAYS

Chen Wu
Defense Research and Development Canada–Ottawa
3701 Carling Av.
Ottawa, Canada, K1A 0Z4

ABSTRACT: *A suspended microstripline-fed linear tapered slot antenna element and its E-plane linear arrays are presented in this paper. The element is studied and designed using the finite-difference time-domain (FDTD) method. The simulated results show that the element has a good antenna performance from 17 to 24 GHz. To build the E-plane arrays, a unique five-piece assembled structure which guarantees a uniform air-filled thin substrate in the suspended microstrip line parallel feed-network, has been developed. Four E-plane arrays with different numbers of elements (4, 8, 16, and 32) are fabricated and their antenna gains and patterns are examined experimentally.* © 2004 Wiley Periodicals, Inc. Microwave Opt Technol Lett 41: 451–455, 2004; Published online in Wiley InterScience (www.interscience.wiley.com).
DOI 10.1002/mop.20168

Key words: *microstrip antenna; tapered slot antenna; microstrip antenna array; suspended microstrip line*

1. INTRODUCTION

The characteristics of the linear tapered slot antenna (LTSA) have drawn a lot of attention among antenna designers. The LTSA is a broadband element that can have high element gain and close E- and H-plane beamwidths; thus, it is a good element for the design of antenna arrays [1–3]. The waveguide-to-finline transition [4] was the early feeding technique used to feed the element. As printed antennas and microwave integrated circuits became more popular, a number of feeding structures have been created. In [5], an excellent review of these designs was given. Since then, a number of new feeding structures has been developed for various applications. Some examples are given in [6, 7]. Although a

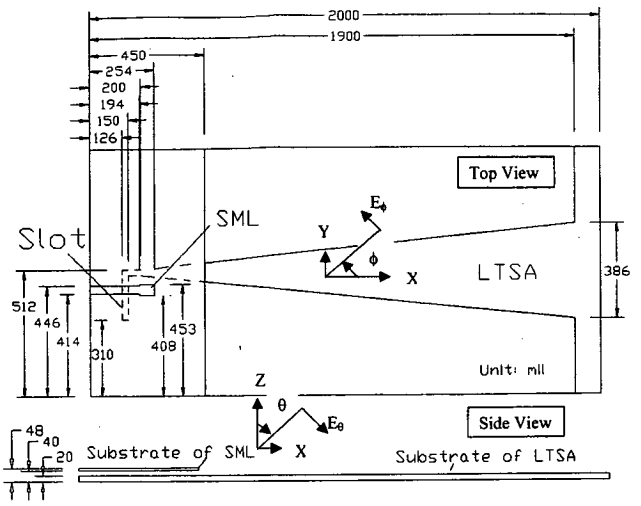

Figure 1 LTSA element fed by the SML

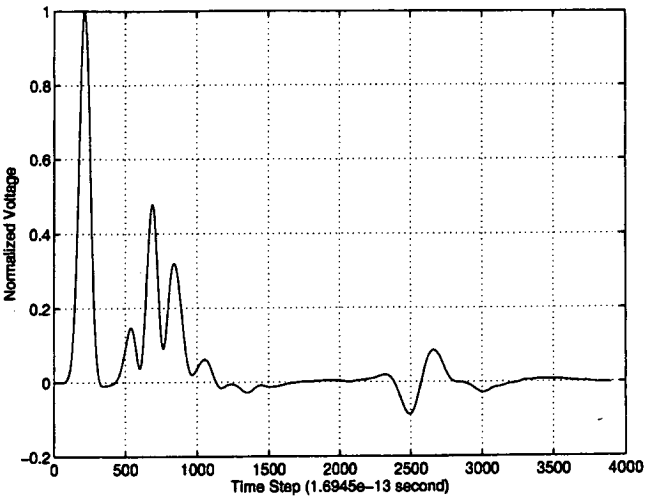

Figure 2 Time-domain signal sampled at the input port of the SML

microstrip-to-slot transition is one of the simplest feeding structures to feed an LTSA, the loss in the microstrip beam-forming network (BFN) is always a major concern when an array is designed in microwave and millimeter-wave frequency bands. To reduce the loss in a BFN and maintain low cost when building an array, the microstripline can be replaced by a suspended microstripline (SML). In general, an SML has lower loss than a microstripline, since a greater portions of the fields exists in the air slab. A broader linewidth is possible for prescribed characteristic impedance. To build E-plane arrays, an assembled five-piece SML-fed LTSA structure is designed and presented in this paper. In this structure, a stamped copper sheet is used as a spacer to create a thin air layer in the SML BFN. The advantages of the structure are: (i) inexpensive substrates can be used to build arrays, and (ii) the parasitic radiation from the SML BFN is eliminated. An LTSA element and its SML-to-slot transition are designed and optimized using the finite-different time-domain (FDTD) method. E-plane linear arrays are fabricated and tested using N elements (N = 4, 8, 16, and 32). The measured results demonstrate that these arrays have a good antenna performance from 17 to 24 GHz.

2. ANTENNA ELEMENT AND FDTD SIMULATION RESULTS

The LTSA element and its dimensions are shown in detail in Figure 1. In the figure, a V slot and a slot line are etched in the ground plane of SML. The ground plane is supported by an FR4 substrate with thickness of 20 mil. An SML is printed on a Rogers RO4003 board, and the substrate thickness is 8 mil. The characteristic impedance of the SML is about 100Ω [8]. The size of the V slot's open end is about one-half of a free-space wavelength at 17 GHz. By changing the slot line's length and width, and the size of the small patch at the end of the SML, the SML-to-slot transition is optimized to operate in the K-band. The computational domain of the FDTD method is a rectangular box, and the cell numbers are 582, 370, and 119 in the X, Y, and Z directions, respectively. The cell size ($dx = dy = dz$) is 4 mil. On the six boundaries of the computational domain, an 8-layer perfectly matched layer (PML) was used to simulate antenna in the free space. To investigate the reflections from different discontinuities of the element, a time-domain signal was sampled on the SML feed line. The sampling point was 300 mil away from the slot line. The sampled time-domain signal is shown in Figure 2. The first peak, between 0 and $370\Delta t$ ($\Delta t = 1.6945 \times 10^{-13}$ s), is the incident Gaussian pulse. After the incident wave passes through the sampling point, the reflected waves begin to arrive. The SML-to-slot transition and the beginning portion of the V slot are the main discontinuities that create the reflected waves between $370\Delta t$ and $2000\Delta t$. The reflected wave shown around $2500\Delta t$ is the wave bounced back from the open end of the element. Using the pulse from 0 to $370\Delta t$ as the incident wave and from $370\Delta t$ to $2000\Delta t$ as the reflected waves, one can obtain the return loss (Fig. 3) of the transition calculated with a V slot. It is obvious that the transition has a good bandwidth, which center frequency is around 20 GHz. Figure 4 depicts the calculated return loss of the element, taking into account all the reflected waves. Although there are multireflections from different discontinuities, the return loss of the element is less than −10 dB in the K-band. The calculation of the return loss shown in this section also demonstrates that the FDTD method is a useful design tool that can be used to de-interleave and analyze multireflections caused by the different discontinuities in an antenna structure. In Table 1, the measured and simulated E- and H-plane antenna beamwidths are listed. From the table, one can find that:

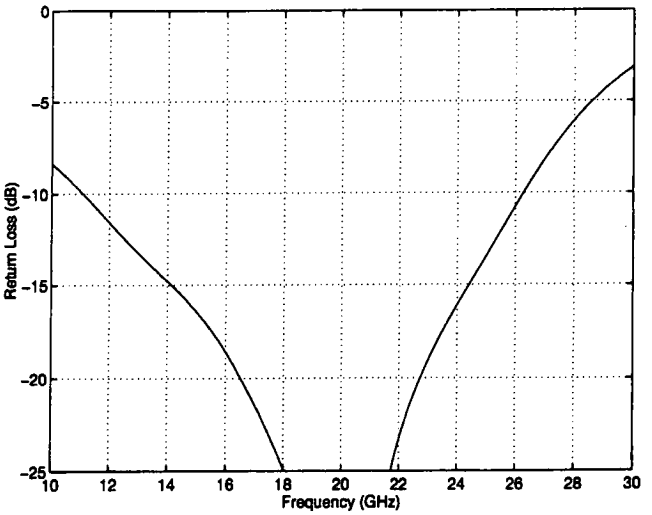

Figure 3 FDTD-simulated return loss of the SML-to-slot transition calculated with the V slot, which is the beginning portion of the LTSA

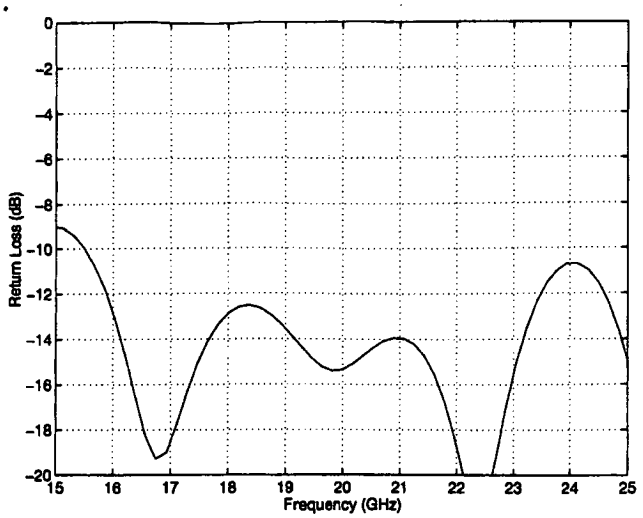

Figure 4 FDTD-simulated return loss of the LTSA element

1. the measured and simulated beamwidths are in good agreement;
2. as frequency increases, the beamwidths become narrower in both E- and H-planes;
3. as frequency increases, the difference between E- and H-plane beamwidths tends to become smaller.

The third result agrees with the general conclusion that for a long LTSA (length > ~3 wavelength) the E- and H-plane beamwidths can be very close to each other.

3. ARRAY STRUCTURE

N-element (N = 4, 8, 16, and 32) E-plane linear arrays were designed and fabricated using the element described in the last section. The inter-element spacing was 486 mil. Figure 5 shows a photo of the five components used to assemble two 16-element linear arrays and a portion of the assembled array. From top to bottom, the components shown in Figure 5 are:

1. Back plate (thickness = 200 mil), which is used to support the array structure;
2. Single-sided copper-printed FR4 board (thickness = 20 mil)—the copper-printed surface acts as the ground plane of the SML, and slot lines and LTSA elements are etched in the surface;
3. Copper spacer (thickness = 20 mil), which has copper islands—these copper islands are the spacers, and air gaps among the islands form the air-filled slab in the SML;
4. Rogers RO4003 board (thickness = 8 mil), upon which the SML BFN is printed;
5. Aluminum cover (thickness = 300 mil), which covers the BFN in order to reduce parasitic radiation from the BFN.

TABLE 1 Simulated and Measured E- and H-Plane Beamwidths at 17, 21, and 24 GHz

Radiation Plane	E-plane			H-plane		
Frequency (GHz)	17	21	24	17	21	24
Simulated beamwidth (°)	44.0	37.0	30.5	37.2	34.0	31.3
Measured beamwidth (°)	46.0	39.0	32.0	36.0	33.0	30.0

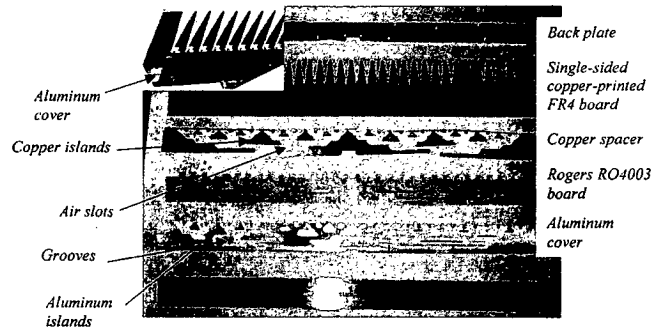

Figure 5 Five components used to build two 16-element LTSA subarrays and a portion of the assembled array

Grooves (with depth of 250 mil) were engraved on the inside surface of the cover. Two alignment pins were used to ensure that the five components were well aligned. Once the array was assembled, the aluminum cover and back plate squeezed the other pieces together by a number of screws. Since the pattern of the aluminum islands on the cover is the same as that of the copper islands in the spacer (Fig. 6), the cover places uniform pressure on the spacer when the array is assembled. Because the copper spacer is stamped from a copper sheet with 20-mil thickness and ±0.5-mil tolerance, a uniform air slab was formed in the SML by the spacer. Two 1-to-16 printed parallel-feed networks are shown in Figure 6. The parallel-feed network creates a uniform weighting among the 16 elements. A 50Ω to 100Ω T-junction and a two-section 100Ω to 50Ω impedance transformer were designed by the FDTD method and used in the SML BFN. The input port of each array was connected to an SMA connector. An HP8510 network analyzer was used to measure the return losses and antenna patterns.

4. MEASURED RESULTS

The measured beamwidths and gains of the linear arrays are listed in Table 2. G_c is the predicted gain, calculated by

$$G_c = \textit{measured element gain} + 3*(\log N/\log 2),$$

where N is equal to 4, 8, 16, and 32. From the table, one can observe the following.

1. The maximum gain difference ΔG ($= G_c - G$) between the measured and predicted gains of different arrays at different frequencies is 1.8 dB. The errors are mainly contributed by:
   a. a loss in the SML BFN;
   b. a small mismatching at the T-junctions and impedance transformers in the SML BFN;
   c. the connection between the SMA connector and SML port;
   d. misalignment between the slots on the FR4 board and the SML feed-lines on RO4003 board.
2. The H-plane beamwidths of the arrays are close to the beamwidths of the single element at different frequencies.

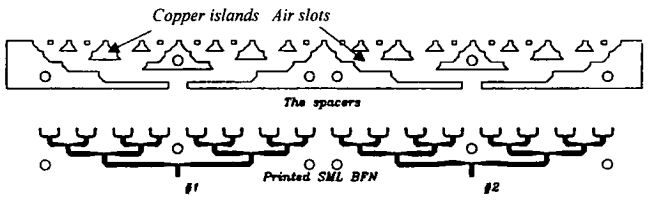

Figure 6 Pattern of the copper spacer and printed SML parallel-feed network on Rogers RO4003 board

TABLE 2 Measured E- and H-Plane Beamwidths and Gains of Arrays with 4, 8, 16, and 32 Elements at 17, 21, and 24 GHz

N		1			4			8			16			32		
F (GHz)		17	21	24	17	21	24	17	21	24	17	21	24	17	21	24
BW (°)	E	46	39	32	19	16	13	8.7	7.8	6.3	4.4	3.6	3.2	2.2	1.8	1.6
	H	36	33	30	37	34	31	38	35	31	38	34	31	38	36	30
G (dBi)		9.5	9.7	10.1	15.0	14.8	15.0	17.2	18.6	19.1	19.7	20.9	21.5	22.8	23.2	24.1
G_c (dBi)		—	—	—	15.5	15.7	16.1	18.5	18.7	19.1	21.5	21.7	22.1	24.5	24.7	25.1
$\Delta G = G_c - G$		—	—	—	0.5	0.9	1.1	1.3	0.1	0	1.8	0.8	0.6	1.7	1.5	1.0

BW: beamwidth, E: E plane, H: H plane, G: measured gain, G_c: measured element gain plus 3 dB * (log$N$/log2), N = 4, 8, 16, 32.

The measured return losses of two 16-element arrays show in Figure 7. It can be seen that they have a good consistency from 17 to 24 GHz, and are less than −10 dB at most frequencies. Using an external 3-dB power combiner and two short cables, a 32-element array was built using two 16-element subarrays, and measured using an HP network analyzer. Since radiation patterns have good symmetry, half of the measured E- and H-plane co- and cross-polarization patterns at 17 and 24 GHz are drawn in Figures 8(a) and 8(b), respectively. These measured patterns show that the array has very low cross-polarization levels. Although it is a uniform weighted array, the sidelobes decay faster than other uniform weighted arrays. This is because the E-plane pattern of the element decays faster than other elements (for example, patch and dipole antennas) when the radiation angle is away from the broadside of the array. It can be found from the measured patterns that the front-to-back ratios of the 32-element array are better than 50 and 45 dB at 17 and 24 GHz, respectively. The main reason why the low cross-polarization level and the high front-to-back ratio are obtained is that the aluminum cover shields the parasitic radiation from the SML feed network, and somehow the back plate and aluminum cover block the array radiating to the angles opposite to the broadside of the array.

CONCLUSION

A printed LTSA element fed by the SML has been designed using the FDTD method. E-plane linear arrays with different numbers of elements (4, 8, 16, and 32) were studied experimentally. The simulated and measured results show that the element and arrays have a wide operating bandwidth. A 32-element E-plane linear array was built using two 16-element subarrays, an external 3-dB power combiner, and two short RF cables. The array demonstrates good antenna gain, symmetrical patterns, low cross-polarization levels, low sidelobes, and high front-to-back ratios at different frequencies. A five-piece assembled antenna structure has been designed to build these arrays. The advantages of the structure are: (i) it guarantees a uniform air slab in the SML BFN, (ii) inexpensive substrates can be used to build arrays, and (iii) it eliminates the parasitic radiation from the SML BFN. In another work, a 32 × 32-element array was built using thirty-two 32-element E-plane linear arrays with an H-plane SML BFN [9]. The array demonstrated good antenna gains and patterns from 17 to 24 GHz and can be used in point-to-point and point-to-multipoint communications.

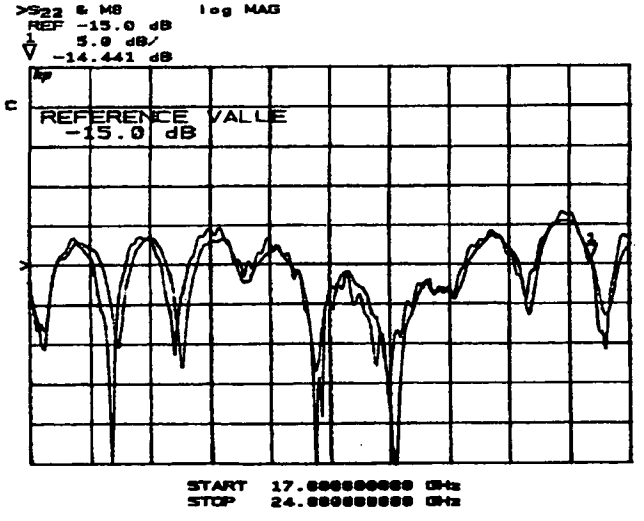

Figure 7 Measured return losses of two 16-element subarrays

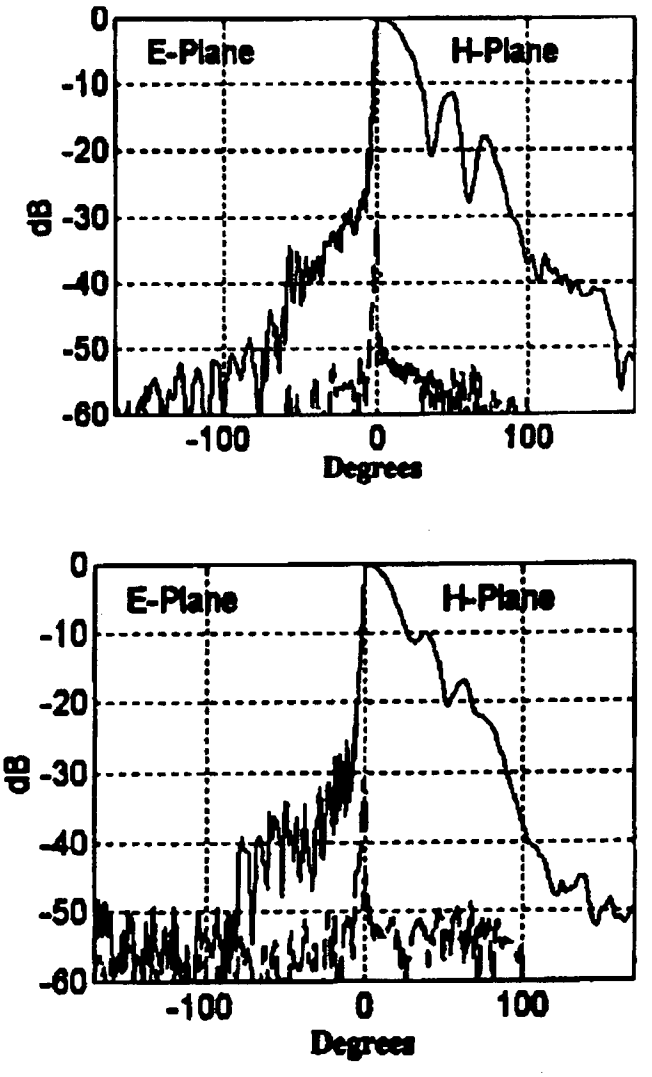

Figure 8 Measured co- and cross-polarization patterns of the 32-element array in the E- and H-planes: (a) 17 GHz; (b) 24 GHz

ACKNOWLEDGMENT

The author would like to thank Dr. Jim P. Y. Lee of Defence Research and Development Canada–Ottawa, and Dr. John Litva of TenXc Inc., Ottawa, Canada, for their encouragement and great support, and Dr. Yifeng Zhou of Defence Research and Development Canada–Ottawa, for a number of good discussions and suggestions.

REFERENCES

1. K.S. Yngvesson, D.H. Schaubert, T.L. Korzeniowski, E.L. Kollberg, T. Thunhren, and J.F. Johasson, Endfire tapered slot antennas on dielectric substrates, IEEE Trans Antennas Propagat AP-33 (1985), 1392–1400.
2. K.S. Yngvesson, T.L. Korzeniowski, Y.S. Kim, E.L. Kollberg, and J.F. Johansson, The tapered slot antenna—a new integrated element for millimeter-wave applications, IEEE Trans Microwave Theory Tech MTT-37 (1989), 365–374.
3. Y.S. Kim and K.S. Yngvesson, Characterization of tapered slot antenna feeds and feed arrays, IEEE Trans Antennas Propagat AP-38 (1990), 1559–1564.
4. A. Beyer, Millimeter-wave antenna in finline technique, ICAP'83, 1983, pp. 44–46.
5. R.Q. Lee and R.N. Simons, Linearly tapered slot antenna and feed networks, Antenna Applic Symp, 1994.
6. R.N. Simons, N.I. Dib, R.Q. Lee, and L.P.B. Katehi, Integrated uniplanar transition for linearly tapered slot antenna, IEEE Trans Antennas Propagat AP-43 (1995), 998–1002.
7. J.B. Muldavin and G.M. Rebeiz, MM-wave tapered slot antennas on synthesized low permittivity substrates, IEEE Trans Antennas Propagat AP-47 (1999), 1276–1280.
8. P. Pramanick and P. Bhartia, Computer-aided design models for millimeter-wave fin lines and suspended substrate microstrip lines, IEEE Trans Microwave Theory Tech MTT-33 (1985), 1429–1435.
9. C. Wu, Use of the finite-difference time-domain method to study broadband antennas for millimeter wave point-to-point and point-to-multipoint communications, Ph.D. dissertation, McMaster University, Hamilton, Ontario, Canada, 2000.

A VERY COMPACT ELECTROMAGNETIC BANDGAP STRUCTURE FOR SUPPRESSING SURFACE WAVES IN INTEGRATED CIRCUITS

Yunqi Fu, Naichang Yuan, and Guohua Zhang
School of Electronic Science and Engineering
National University of Defense Technology
Changsha, Hunan Province 410073, P. R. China

Received 25 November 2003

ABSTRACT: *A very compact electromagnetic bandgap structure is presented for integrated-circuits applications. This structure, which is one kind of high-impedance surface with periodic interdigital elements, is adopted to increase the fringe capacitor in order to compress the overall size of the high-impedance surface. Its design uses the effective-circuit model. The measured results show that a 30% to 40% size reduction can be obtained. This will be very valuable for practical applications.* © 2004 Wiley Periodicals, Inc. Microwave Opt Technol Lett 41: 455–457, 2004; Published online in Wiley InterScience (www.interscience.wiley.com). DOI 10.1002/mop.20169

Key words: *EBG; interdigital capacitor; high-impedance surface; surface-wave*

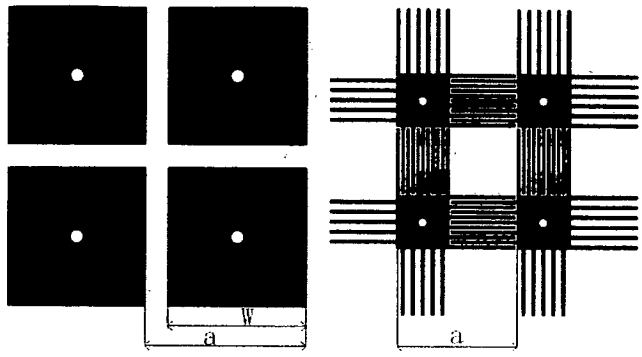

Figure 1 Geometry of the structure's layout of HIP

1. INTRODUCTION

In recent years, photonic bandgap (PBG)/electromagnetic bandgap (EBG) structures have been extensively studied in the applications of microwave circuits and antennas [1–7], and so-called high-impedance surfaces (HIPs) [1–4] have attracted even more attention. HIPs process the two advantages of high surface impedance and in-phase reflected plane wave, whereas the reflected plane wave from a metal sheet is out of phase. Second, it shows a frequency bandgap within which the propagation of surface waves is forbidden. HIPs have been used as microwave antennas, such as the wire antenna microstrip patch antenna [3–4]. Another merit of HIP surfaces is their compact sizes. The periodic spacing can be about one-tenth of the guided wavelength for two-layer HIPs, and for three-layer HIPs, it can be one-thirtieth of guided wavelength [2]. The two-layer structures are more easily integrated into printed circuits using normal MMIC techniques than into three-layer structures. But when the layout of the components is required to be very compact, the two-layer structures will still be too massive.

In this paper, the concept of interdigital capacitors has been introduced to the design of two-layer HIPs. The connection of two adjacent elements creates an interdigital structure, which results in a larger fringe capacitor; hence, a very compact HIP can be obtained for much lower frequencies. The effective-circuit model is used in the design procedure. Several samples have been manufactured and the measured propagation parameters of the surface wave have been given. The measured results shows that this new type of HIP is prospectively useful for realizing more compact size.

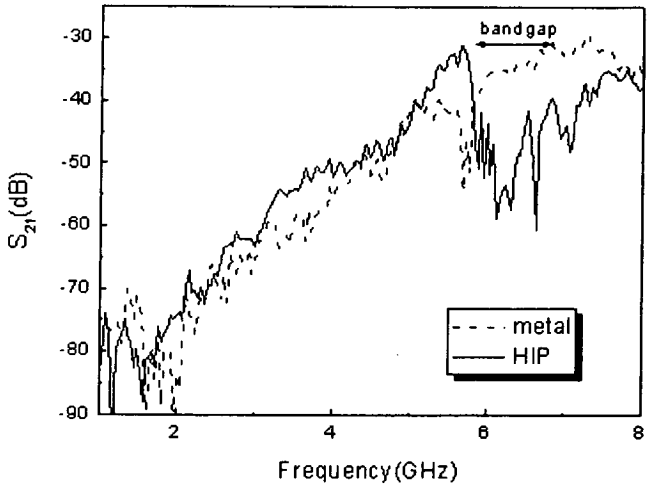

Figure 2 Measured S_{21} of the TM surface wave of C-HIP 1